Adjoint sensitivity of episodic ozone in the Paris area to emissions on the continental scale

Hauke Schmidt, Daniel Martin

Adjoint sensitivity of episodic ozone in the Paris area to emissions on the continental scale

Hauke Schmidt[1]
Laboratoire de Météorologie Dynamique, Ecole Polytechnique, Palaiseau, France

Daniel Martin[2]
Institut Pierre Simon Laplace, Paris, France

Received 10 December 2001; revised 5 June 2002; accepted 5 June 2002; published 29 May 2003.

[1] This study presents results of sensitivity calculations with the adjoint of the continental-scale Eulerian chemistry transport model CHIMERE. In the framework of the Atmospheric Pollution Over the Paris Area (ESQUIF) project, which was designed to improve the understanding of photochemical pollution events in the Paris region, a large number of aircraft and surface observations was performed in order to study the chemical composition around the agglomeration. Here the adjoint CHIMERE model is used to calculate sensitivities of ozone concentrations, in particular of air masses entering the Paris region, with respect to emissions on the continental scale. For 13 case studies the influence of ozone precursors, differentiated with respect to their source type, their geographical origin, and their time of emission, is quantified with the aim of facilitating the interpretation of the observations and to demonstrate the usefulness of adjoint models for such types of studies. It is shown that for all cases the regional peak ozone concentrations are more sensitive to emissions of NO_x than to emissions of volatile organic compounds (VOCs). However, the influence of VOCs is extended over a longer time span than for NO_x, which is reflected in the more distant source regions of highly influential VOC emissions. On average the sensitivity to biogenic VOCs is significantly smaller than to anthropogenic VOCs. The same is true for NO_x emissions. However, as different uncertainties have to be associated with these four emission groups, the uncertainty of the modeled ozone concentration caused by the groups is of the same order of magnitude. *INDEX TERMS:* 0345 Atmospheric Composition and Structure: Pollution—urban and regional (0305); 0368 Atmospheric Composition and Structure: Troposphere—constituent transport and chemistry; 3210 Mathematical Geophysics: Modeling; *KEYWORDS:* adjoint modeling, tropospheric ozone, air quality modeling, ensitivity studies, Paris, precursor emissions

Citation: Schmidt, H., and D. Martin, Adjoint sensitivity of episodic ozone in the Paris area to emissions on the continental scale, *J. Geophys. Res.*, *108*(D17), 8561, doi:10.1029/2001JD001583, 2003.

1. Introduction

[2] Episodic events of high ozone concentrations remain a major pollution concern in different regions of western Europe, though the emissions of the main precursors, NO_x and volatile organic compounds (VOCs), have been reduced significantly since the beginning of the 1990s [*Vestreng and Storen*, 2000]. The Atmospheric Pollution Over the Paris Area (ESQUIF) project [*Menut et al.*, 2000a] was designed to improve the understanding of the formation of photochemical air pollution in one of these regions: in and around the city of Paris, France. A large amount of mostly airborne trace gas observations were made to this end during different episodes of elevated ozone concentrations in 1998 and 1999. Modeling studies like this one are intended to facilitate the interpretation of the observations. It has been recognized earlier [*Vautard et al.*, 1999] that photochemical smog episodes in the Paris area are influenced not only by local emissions but also to a varying degree by the advection of air masses which have already been charged with photooxidants or precursors during their travel over the European continent.

[3] A review of photochemical modeling activities in general is given by *Russell and Dennis* [2000]. This study uses the adjoint model of the three-dimensional (3D) Eulerian chemistry transport model of the boundary layer CHIMERE-continental [*Schmidt et al.*, 2001] to calculate sensitivities of the ozone concentration of air masses enter-

[1]Now at Max-Planck-Institute for Meteorology, Hamburg, Germany.
[2]Now at Météo France, Direction Générale/Environnnement Atmosphérique, Paris, France.

0148-0227/03/2001JD001583

ing and leaving the Paris area to emissions on the European scale. The calculations are made for 13 summer days with elevated ozone concentrations in the years 1998 and 1999. The main question which is addressed is, How large is the sensitivity of ozone smog in Paris to precursor emissions from different European regions and what is the timescale of the sensitivity? Special emphasis is given to the distinction between VOC and NO_x emissions and, within these groups, between anthropogenic and biogenic sources. Assuming that the model is sufficiently realistic, the sensitivities can give an idea of the effects of emission control. On the other hand, they quantify the effect of uncertainties in emissions on the simulation results and may be helpful in the search for possible sources of model errors.

[4] "Classical" sensitivity studies are performed using a "twin simulation" approach, where the influence of a perturbed parameter on the model result is examined. In the context of air pollution modeling this is frequently applied to study the benefits of emission reductions. Nevertheless, if the separate influence of the perturbation of different parameters (such as the reduction of numerous emitted species in different areas) is to be studied, a single model run for each parameter is necessary. A computationally efficient method for these cases is the application of an adjoint model which allows the calculation of gradients (sensitivities) of a model result with respect to an unlimited number of parameters in one model run. However, adjoint models can only calculate first-order sensitivities. Given a nonlinear model, the validity of the sensitivities for large parameter variations is therefore limited.

[5] The application of adjoint equations to meteorological and oceanographical problems is not new and was apparently suggested by *Marchuk* [1974]. It started to become popular in the context of variational meteorological data assimilation in the mid-1980s [*Lewis and Derber*, 1985; *Talagrand and Courtier*, 1987], where the computationally efficient calculation of gradients of a cost function via the adjoint of the local tangent linear equations of the assimilating model is prerequisite. First applications of the variational assimilation technique to atmospheric chemistry models are described by *Fisher and Lary* [1995] for the stratosphere and by *Schmidt* [1999] and *Elbern and Schmidt* [2001] for the troposphere. *Cho et al.* [1987] were probably the first to use adjoint sensitivity calculations in an atmospheric chemistry context, namely to quantify sensitivities of sulfate formation. Later, *Gao et al.* [1995] studied sensitivities of the Regional Acid Deposition Model (RADM) gas phase mechanism. For a simplified model of the Paris area, built of five boxes, *Menut et al.* [2000b] calculated adjoint sensitivities of ozone and nitrogen dioxide with respect to emissions and chemical reaction rates. One of their results is that, depending on the meteorological conditions, ozone in the Paris area might have a positive or negative sensitivity to local NO_x emissions. This paper can be regarded as complementary to the latter study, presenting the influence of emissions on a European scale on ozone around Paris with a full 3D Eulerian model.

[6] The structure of the paper is as follows. Sections 2–4 present background information for the sensitivity experiments, namely the mathematics of adjoint modeling, the model system, and the experimental setup. Section 5 is dedicated to a comparison of observed and simulated ozone concentrations, performed in order to evaluate the model performance. The results of the adjoint model runs are given in section 6, and a summary and discussion are given in section 7.

2. Mathematical Background of Adjoint Modeling

[7] As indicated in section 1, the use of adjoint equations in the simulation of atmospheric or oceanographic processes is not a new idea. Several publications show how the integration of an adjoint model backward in time results in a partial gradient of a scalar function of the model result, which can be interpreted as a sensitivity or which can be used in the minimization process of variational data assimilation. The adjoint equation can be deduced by means of the theory of Lagrangian multipliers, as is done in the context of data assimilation, for example, for initial value optimization by *Daley* [1991] or for emission optimization by *Elbern et al.* [2000]. The presentation here uses the theory of adjoint operators and follows the ideas of *Talagrand and Courtier* [1987] and of *Menut et al.* [2000b].

[8] Consider a time-discretized numerical model, where $\mathbf{x}_n$ is a vector describing the physical state at time t_n and where the time evolution is governed by the equation $\mathbf{x}_{n+1} = M_n(\mathbf{x}_n, \mathbf{y})$. M_n is the (in general nonlinear) model operator for the respective time step and $\mathbf{y}$ is a vector containing a set of parameters. Consider further a scalar function $\mathcal{J}: \mathbf{x}_n \rightarrow \mathcal{J}(\mathbf{x}_n)$, which we assume for the sake of simplicity depends on the model state at only one time step. The aim is to find an expression for the partial gradient of $\mathcal{J}$ with respect to $\mathbf{y}$ which we interpret as a sensitivity S:

$$S = \nabla_{\mathbf{y}} \mathcal{J}(\mathbf{x}_n). \tag{1}$$

Given scalar products in the parameter and in the state space (indicated by $\langle\ \rangle_{\mathbf{y}}$ and $\langle\ \rangle_{\mathbf{x}}$, respectively), a perturbation $\delta\mathcal{J}$ of the scalar function caused by a perturbation of the parameters or of the model state can be written as

$$\delta\mathcal{J}(\mathbf{x}_n) = \langle S, \delta\mathbf{y} \rangle_{\mathbf{y}} \tag{2}$$

or

$$\delta\mathcal{J}(\mathbf{x}_n) = \langle \nabla_{\mathbf{x}} \mathcal{J}(\mathbf{x}_n), \delta\mathbf{x}_n \rangle_{\mathbf{x}}, \tag{3}$$

whereas at any time t_n the time evolution of a perturbation of the model state follows the governing equation

$$\delta\mathbf{x}_{n+1} = \left(\frac{\partial M_n}{\partial \mathbf{x}} (\mathbf{x}_n, \mathbf{y}) \delta\mathbf{x}_n \right) + \left(\frac{\partial M_n}{\partial \mathbf{y}} (\mathbf{x}_n, \mathbf{y}) \delta\mathbf{y} \right). \tag{4}$$

Assuming that there is no initial perturbation of the model state ($\delta\mathbf{x}_o = 0$), a successive application of equation (4) leads to an expression for the perturbation of the model state caused by a perturbation of the parameters during a model run from time t_0 to t_n:

$$\delta\mathbf{x}_n = \sum_{i=1}^{n-1} \left(\prod_{j=n-1}^{i} \mathbf{M}_{\mathbf{x},j} \right) \mathbf{M}_{\mathbf{y},i-1} \delta\mathbf{y} + \mathbf{M}_{\mathbf{y},n-1} \delta\mathbf{y}, \tag{5}$$

where $\mathbf{M}_{\mathbf{x},n}$ and $\mathbf{M}_{\mathbf{y},n}$ denote the partial derivatives of the model operator M_n with respect to $\mathbf{x}$ and $\mathbf{y}$, respectively. $\mathbf{M}_{\mathbf{x},n}$ is, in general, referred to as the tangent linear model operator. Introducing equation (5) into equation (3) and applying the definition for adjoint operators, one obtains

$$\delta\mathcal{J}(\mathbf{x}_n) = \left\langle \left(\sum_{i=1}^{n-1} \mathbf{M}^*_{\mathbf{y},i-1} \prod_{j=i}^{n-1} \mathbf{M}^*_{\mathbf{x},j} + \mathbf{M}^*_{\mathbf{y},n-1} \right) \nabla_{\mathbf{x}}\mathcal{J}(\mathbf{x}_n), \delta\mathbf{y} \right\rangle_{\mathbf{y}}, \tag{6}$$

where the asterisk denotes the adjoint operators. Comparison with equation (2) shows that the expression left of the comma inside the scalar product is the wanted sensitivity S of the function $\mathcal{J}$ with respect to the parameters contained in the vector $\mathbf{y}$. As the adjoint operators are linear, S can be calculated by a single successive application of the adjoint tangent linear model operators $\mathbf{M}^*_{\mathbf{x},j}$ (backward integration of the adjoint model), with the gradient $\nabla_{\mathbf{x}}\mathcal{J}(\mathbf{x}_n)$ as initial condition and the results of the application of the operators $\mathbf{M}^*_{\mathbf{y},i}$ summed up for every time step. Following the same argument, the calculation of a sensitivity for a scalar function depending on the model state at all time steps and not only at t_n is straightforward.

3. CHIMERE Model System

3.1. Basics of the Model Formulation

[9] CHIMERE is a Eulerian 3-dimensional chemistry transport model (CTM) of the boundary layer which is mainly intended for real-time forecasts (see http://euler.lmd.polytechnique.fr/pioneer) and long-term simulations. It consists of a European-scale model with a horizontal resolution of $0.5° \times 0.5°$ [*Schmidt et al.*, 2001] and of different nested regional models [*Vautard et al.*, 2001]. In this study, only the continental-scale model is used, for which an adjoint model has been developed. In this section a brief description of the main characteristics of the model is given. Only the emission modeling is presented more exhaustively in section 3.2, as the study concentrates on the sensitivity of ozone concentrations to emissions. For more details of the other model features and for an evaluation of the model performance for the summer of 1998, see *Schmidt et al.* [2001].

[10] The horizontal model domain is given in Figure 1. In the vertical the model contains five levels defined by hybrid coordinates up to 725 hPa. As characteristic of the Eulerian approach, the model is based on the mass continuity equation for a number of chemical species in every box of the given grid [e.g., *Seinfeld and Pandis*, 1998]. The numerical method for the temporal solution of the stiff system of partial differential equations is adapted from the second-order TWOSTEP algorithm which was originally proposed by *Verwer* [1994] for gas phase chemistry only, but here it is applied to the complete system of equations [*Schmidt et al.*, 2001]. The frequently used operator-splitting technique is avoided by this approach. It is applied in this study with a relatively long time step of 10 min and only one Gauss-Seidel iteration, which introduces a slight degradation of the accuracy but, owing to the implicit character of TWOSTEP, no stability problems. Chemical production and loss terms are calculated with the Modele Lagrangien de Chimie de l'Ozone a l'echelle Regionale (MELCHIOR) mechanism [*Lattuati*, 1997], which contains in the reduced form applied here [*Schmidt et al.*, 2001] 44 chemical species and 116 reactions. The hydrocarbon degradation is similar to the European Monitoring and Evaluation Programme (EMEP) gas phase mechanism [*Simpson*, 1992]. (The complete list of chemical species and reactions can be found at http://euler.lmd.polytechnique.fr/chimere.)

[11] Meteorological input to force the model is taken from European Centre for Medium-Range Weather Forecasts (ECMWF) model outputs every 3 hours with spectral resolutions of T319, corresponding to a grid size of $\sim 0.5°$. Horizontal advective transport is usually calculated with the piecewise parabolic method (PPM) approach [*Carpenter et al.*, 1990], which, for this study, is replaced by a simple first-order technique (see section 3.3). Vertical diffusion is based on an eddy diffusion approach, with coefficients calculated using a profile after *O'Brien* [1970]. Deposition of trace gases is modeled following the resistance analogy presented by *Wesely and Hicks* [1977] and by *Erisman et al.* [1994]. Boundary concentrations for species with longer lifetimes are taken from a climatology of the global Model of Ozone and Related Trace Species (MOZART) [*Hauglustaine et al.*, 1998]. Initial concentrations are taken from preceding model runs over a spin-off time of at least 4 days.

3.2. Emissions

[12] The model requires input emission data for 14 model species. Annual data of anthropogenic emissions for the four classes NO_x, SO_2, CO, and nonmethane volatile organic compounds (NMVOC) are taken from the EMEP database for 1998 [*Mylona*, 1999] (see also the web site http://www.emep.int). The data are spatially interpolated from the EMEP grid onto the CHIMERE grid. The NMVOC emissions have to be split into eight classes, represented within the model's chemical mechanism. To this end, they are first distributed for each country into different activity sectors (traffic, solvents, industrial and residential combustion, others), according to data prepared by the Institute for Energy Economics and Rational Use of Energy (IER), University of Stuttgart, Germany [*Generation of European Emission Data for Episodes Project* (*GENEMIS*), 1994]). For each sector, NMVOC emissions are then split into 32 classes with similar structure and reactivity, following a classification of *Middleton et al.* [1990] and using VOC profiles, again from IER. Third, VOCs from these 32 classes are aggregated into the 8 classes represented within the model by applying mass and reactivity weighting, as proposed by *Middleton et al.* [1990]. It should be noted that the uncertainty in the spatial distribution of individual VOC emissions is large, given that the VOC profiles are assumed to be the same all over Europe with the exception of traffic, where national differences (e.g., the ratio gasoline/diesel) are taken into account. Monthly, daily, and hourly variations of the emissions are modeled by imposing respective variations from the *GENEMIS* [1994] database.

[13] In rural areas, NO emissions from microbial processes may be an important source of NO_x. In soils, NO is produced in a reaction chain of oxidation and reduction from ammonium used in fertilizers [*Williams et al.*, 1992]. The model uses a European inventory of soil NO emissions from *Stohl et al.* [1996]. This inventory estimates soil

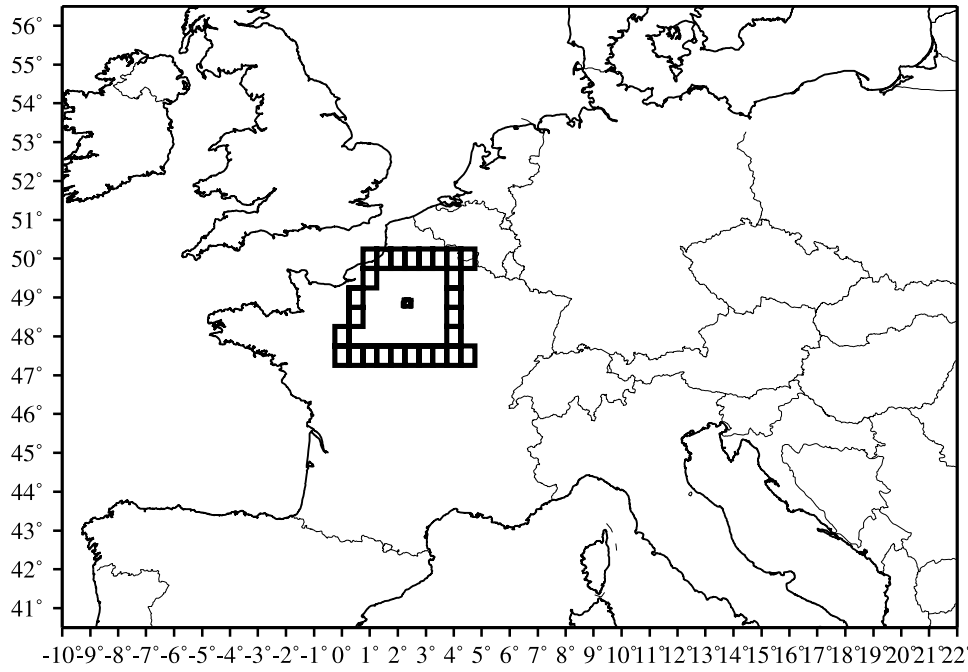

Figure 1. CHIMERE model domain. The model grid boxes are touched by the flight paths of the Météo France aircraft Merlin IV with the exception of flights on 30 July, of which the southern leg was closer to Paris (see Figure 4). The city of Paris is marked as a dot.

emissions to be of the order of ~20% of the emissions from combustion on a European average during the summer months but with large differences between the countries. It should be noted that there is still a high uncertainty concerning these emissions, and some other estimates are much lower [e.g., *Veldkamp and Keller*, 1997]. These NO emissions are sometimes denoted as biogenic. As this term is misleading, in section 3.3, NO_x emissions from combustion (taken from the EMEP inventory) and from soils [*Stohl et al.*, 1996] will be distinguished.

[14] Biogenic emissions of isoprene and terpenes (affected to α-pinene in the chemical mechanism) are parameterized as fluxes $F_i = \epsilon_i D \gamma_i$ [*Guenther*, 1997], with ϵ_i being the species-dependent "emission potential" and D the "foliar density" [from *Simpson et al.*, 1999]. The "environmental correction factor" γ_i accounts for the dependence on temperature and insolation [*Guenther*, 1997]. The spatial distribution of tree species is established following the methodology outlined by *Simpson et al.* [1999]. Therefore the Stockholm Environment Institute (SEI) land cover database, which details the fraction of different tree species over Europe, is interpolated on the CHIMERE grid. The 136 SEI land-use classes are aggregated into 11 "emitter" classes. Oak trees, for example, are differentiated by the classes highly isoprene-emitting, highly terpene-emitting, and low biogenic VOC-emitting. As this attribution of classes is sometimes ambiguous, national tree species inventories from *Simpson et al.* [1999] are used to verify the fraction of each emitter class on a country-wise level and to adjust it, if necessary.

3.3. Adjoint Model

[15] The adjoint of the CHIMERE model was coded line-by-line and by hand, largely following the principles formulated by *Talagrand* [1991] and by *Giering and Kaminski* [1998]. This means that the discretized equations of the direct model were linearized, and then the adjoint was calculated. This is today, to our knowledge, the most frequently used approach for building adjoint code. However, it is also possible to first calculate the adjoint of the analytical direct model equations and then discretize as the second step. Analytical adjoint equations for a Eulerian CTM have been derived by *Elbern and Schmidt* [1999] and for gas phase chemistry only by *Elbern et al.* [1997]. It has been discussed [*Sirkes and Tziperman*, 1997] which approach is the most appropriate. The first approach offers the advantage of leading to an exact adjoint of the direct model, but difficulties with nonlinearities may occur (see section 3.3), and an approximate adjoint might be sufficient for some applications.

[16] The adjoint code has been tested extensively using the method proposed by *Chao and Chang* [1992] and by comparison of the adjoint model results with sensitivities calculated with the classical twin approach with perturbed emissions. Owing to the nonlinearity of the direct model, during the integration of the adjoint model, species concentrations and other variables of the direct model run have to be available. Therefore storage limitations impose frequent recalculations of these variables such that for one adjoint model integration the direct model has to be integrated about 3 times. Nevertheless, the CPU time for a complete adjoint model run with the model configuration described above is ~20 min for a 1-day simulation on a PC.

[17] As noted before, the PPM technique (numerical scheme for horizontal advection) is replaced in this study by a first-order transport scheme. The reason for this is the tendency of higher-order nonoscillatory advection algorithms to produce spatial oscillations in sensitivity fields

Table 1. Target Dates for the Adjoint Sensitivity Experiments

	Wind[a]		Entry		Exit		O_3 Mixing Ratio[b]				
Day	Direction, deg	Speed, m s^{-1}	Latitide, °N	Longitude, °E	Latitude, °N	Longitude, °E	ENT1	EXT1	ENT3	EXT3	Flight[c]
8 Aug 1998	133	3.9	48.0	4.0	49.0	0.5	82	92	81	89	M
9 Aug 1998	121	2.8	48.5	4.0	48.5	0.5	96	103	97	105	M
16 June 1999	52	3.0	50.0	3.5	47.5	1.5	80	74	86	78	
17 June 1999	333	5.3	49.5	1.0	47.5	2.5	61	84	60	89	
25 June 1999	90	4.0	49.5	4.0	48.5	0.5	72	77	76	82	A
26 June 1999	221	6.1	48.0	0.0	49.5	1.0	48	70	52	76	
2 July 1999	181	4.7	47.5	3.5	49.5	1.0	55	61	56	61	A
17 July 1999	139	2.1	48.5	4.0	49.0	0.5	59	66	63	69	A
18 July 1999	174	3.2	47.5	1.5	50.0	2.0	60	74	65	76	M
24 July 1999	64	7.6	49.0	4.0	48.5	0.5	50	56	54	61	
25 July 1999	75	8.1	49.5	4.0	48.5	0.5	59	63	64	68	
29 July 1999	65	4.1	49.5	4.0	47.5	1.0	65	70	69	73	
30 July 1999	56	1.9	49.5	4.0	47.5	1.5	70	82	73	85	M,A

[a]Mean values over 24 hours from European Centre for Medium-Range Weather Forecasts model data for 49.0°N, 2.5°E and 900 m altitude.
[b]Time 15 UTC, modeled by CHIMERE for the respective coordinates at the entry and exit of the Paris region in the surface layer (ENT1, EXT1) and in the third model layer at ~900 m (ENT3, EXT3).
[c]M is morning flight; A is afternoon flight; and no value indicates no flight.

calculated for very small or infinitesimal (as in the adjoint method) perturbations. The meaning of these fields is limited, as the PPM technique shows a strongly nonlinear behavior for such small perturbations. The same problem is described by *Vukićević and Hess* [2000] for another advection scheme. The mathematical description of this behavior and possible solutions are discussed by *Vukićević et al.* [2001] and by *Thuburn and Haine* [2001]. In section 6.5, it will be shown that the application of the more diffusive first-order advection scheme does not qualitatively influence the results of this study.

4. Experimental Setup

4.1. General Disposition

[18] In the framework of the ESQUIF campaign, during ozone pollution episodes of the summer seasons of 1998 and 1999, a large number of airborne trace gas observations was made. One aim was to examine air masses entering and leaving the Paris area. The largest-scale flights were performed by the Météo France aircraft Merlin IV following, at an altitude of ~900 m above sea level, a nearly quadrangular path (see Figure 1) around the agglomeration, with a distance to the center of ~100–150 km. The dates of the eight flights of this type are indicated in Table 1. As the Paris agglomeration is surrounded by relatively unpopulated and unindustrialized areas, the air masses observed at the flight legs upwind of Paris are suspected to reach the agglomeration without being exposed to substantial amounts of additional precursor emissions. The aircraft observations are used in this study to evaluate the model, which is then used for the sensitivity calculations. A detailed description of the observations and of the meteorological and chemical situation is given by the *Atmospheric Pollution Over the Paris Area Project Team* (*ESQUIF*) [2001].

[19] The model, with its horizontal resolution of 0.5° × 0.5°, cannot be expected to correctly simulate the chemical situation in and near Paris. Contrarily, the large-scale Merlin flight path should correspond to the model resolution. The idea behind the numerical experiments of this study is to calculate sensitivities of the ozone concentrations with respect to emissions observed by the flights upwind of Paris. By this means it should be possible to determine the origin of the ozone concentrations which were already well above a background level of, say, 40 ppb when entering the Paris area for all cases (see Table 1). The study is concentrating on ozone, as it was shown that in local-scale modeling of ozone pollution in Paris the most influential species concentration at the boundary of the local model was, by far, that of ozone itself [*ESQUIF*, 2001].

4.2. Different Numerical Experiments

[20] Adjoint model simulations are performed with the scalar function $\mathcal{J}$ (see section 2) being the ozone mixing ratio in one of the model boxes (called the target box) touched by the Merlin flight path at a certain target time for 13 days within the intensive observation periods (IOPs) of ESQUIF. Despite the varying time of the flights, the target time of the main series of experiments is fixed at 15 UTC, being, in general, close to the time of the maximum ozone concentration. This renders the simulations for the different days comparable. In order to base the study on a larger number of cases, experiments are also made for some days with no aircraft observations. The target box is chosen for each experiment with the help of trajectory calculations. It lies on the intersection of the flight path and a trajectory passing over the city of Paris some hours later. All target boxes for this main series of experiments are chosen to be in the third model layer (~600–1200 m), corresponding to the flight altitude.

[21] In order to evaluate the influence of the target time and of the location of the target box on the calculated sensitivities, all experiments are repeated for the target time of 9 UTC and for both times with target boxes in the surface model layer (~0–50 m). A last series of experiments has the target boxes not at the entry, but at the exit, of the Paris region. The boxes were again chosen to be at the intersection of the flight path with trajectories of an air mass having crossed the city of Paris. The comparison of sensitivities calculated for ozone entering and exiting the agglomeration should allow a first estimation of the effect of the Paris emissions itself, though it is evident that a continental-scale model cannot resolve the city plume in all detail.

[22] In total, a set of 8 × 13 adjoint experiments is performed. However, the interpretation will focus on the series of 13 experiments with the target box upwind in the third model layer at 15 UTC. In the following the experiments are labeled as, for example, 1999073015ENT1 (target time: 15 UTC 30 July 1999; target box: entry of the Paris region, model layer 1) and the series of experiments as, for example, 15ENT1 (all experiments with the target time 15 UTC and the respective target box). An overview of the days for which experiments are made together with the mean wind at that day, the coordinates of the target boxes, and the simulated ozone mixing ratios is given in Table 1.

4.3. Details of the Sensitivity Calculations

[23] For each experiment the adjoint model is integrated over ~3.5 days backward in time (87 hours for target time 15 UTC and 82 hours for 9 UTC). The model outputs are gradients $S^{O_3}_{i,j,t}(k)$ of the ozone concentration in the target box and at the target time of experiment k with respect to emissions of model species i during the hour denoted by t in the model grid box with the horizontal index j. Inorganic emissions are considered for the species NO, NO_2, CO, and SO_2, anthropogenic organic emissions for the model species C_2H_6, NC4H$_{10}$ (*n*-butane), C_2H_4, C_3H_6, *o*-xylene (OXYL), HCHO, CH_3CHO, and CH_3COE (methyl ethyl ketone), and biogenic organic emissions for C_5H_8 (isoprene) and α-pinene (APINEN). In the case of NO, emissions of combustion and soil sources are distinguished. To facilitate the interpretation of the experiments, sensitivities are in general given as

$$\tilde{S}^{O_3(k)}_{i,j,t} = E(i,j,t)/100 * S^{O_3(k)}_{i,j,t}, \quad (7)$$

i.e., as products of the gradient with the respective emission value $E(i, j, t)$. The unit of the sensitivities is ppb%, which means that the sensitivity gives the change of the ozone mixing ratio in ppb due to a 1% increase of the emissions of species i in the horizontal grid area j during the hour t. With 15 species, 2145 horizontal grid points, and 87 hours of simulation, nearly 3 million sensitivities are calculated during each adjoint simulation. In the following the results are generally given as integrated values over groups of species, over all modeling hours, or over the complete model domain.

5. Comparison of the Direct Simulations With Observations

[24] If the intention is to interpret the calculated sensitivities not only within the model "reality" but also for the real world, the model has to be sufficiently realistic. To evaluate the performance of the model, a comparison of the simulation results with as many observations as possible is necessary. *Schmidt et al.* [2001] have done this by comparing CHIMERE simulations for the summer of 1998 with mostly ozone observations of more than 100 European surface observation sites. The mean RMS error of the daily maximum ozone concentration for stations not in an urban zone is 9.8 ppb in that study. Nevertheless, *Schmidt et al.* [2001] state that errors are larger for high concentrations and that the model has a slight tendency to underestimate high concentrations. As, for this study, only days with elevated concentrations are selected, errors are expected to be larger than for mean conditions. Recent long-term simulations for the years 1999–2001 show model error statistics similar to those for 1998.

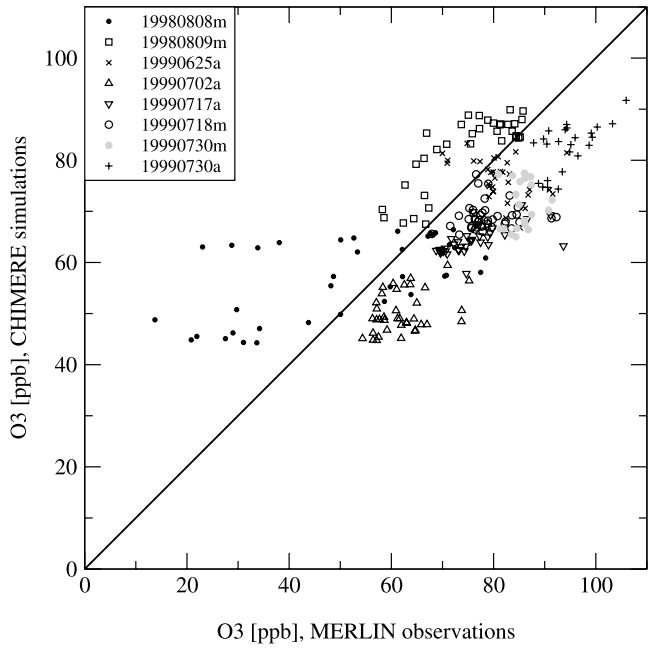

Figure 2. Five-minute mean ozone mixing ratios observed during the eight flights indicated in the legend versus respective simulated mixing ratios which are interpolated in space and time to the respective airplane coordinates. The letters "m" and "a" in the legend indicate morning and afternoon flights, respectively.

[25] In Figure 2, 5-min mean ozone mixing ratios from the Merlin flights are compared to simulations for model layer 3 which are linearly interpolated in space and time. A model tendency to underestimate the observations of 1999 can be discovered as well as a mean overestimation of the observations from the two flights in 1998. The correlation coefficient for all the presented pairs of aircraft observations and simulations is 0.70. Small patches of very clean air with extremely low ozone concentrations were observed during the morning flight on 8 August 1998. The origin of these structures is not yet clear, and they cannot be resolved by the model. The observation was confirmed by a second aircraft flying a different path.

[26] The interpretation of the adjoint simulations will concentrate on the experiments of 17 and 30 July 1999. These dates were chosen because they represent two cases where the air masses entering the Paris region were influenced by emissions of very different regions. Figures 3 and 4 show more detailed comparisons for these days. The observations show little large-scale differences along the flight path, except for two observation peaks around the northwest corner of the flight on 17 July, of which the second can be attributed to the Paris plume. The simulations follow the observed larger-scale patterns. Nevertheless, on both days the ozone mixing ratio is underestimated by ~10 ppb during almost the entire flight. One of the questions to be answered by the adjoint sensitivity calculations is therefore whether errors in emissions are possible reasons for these under-

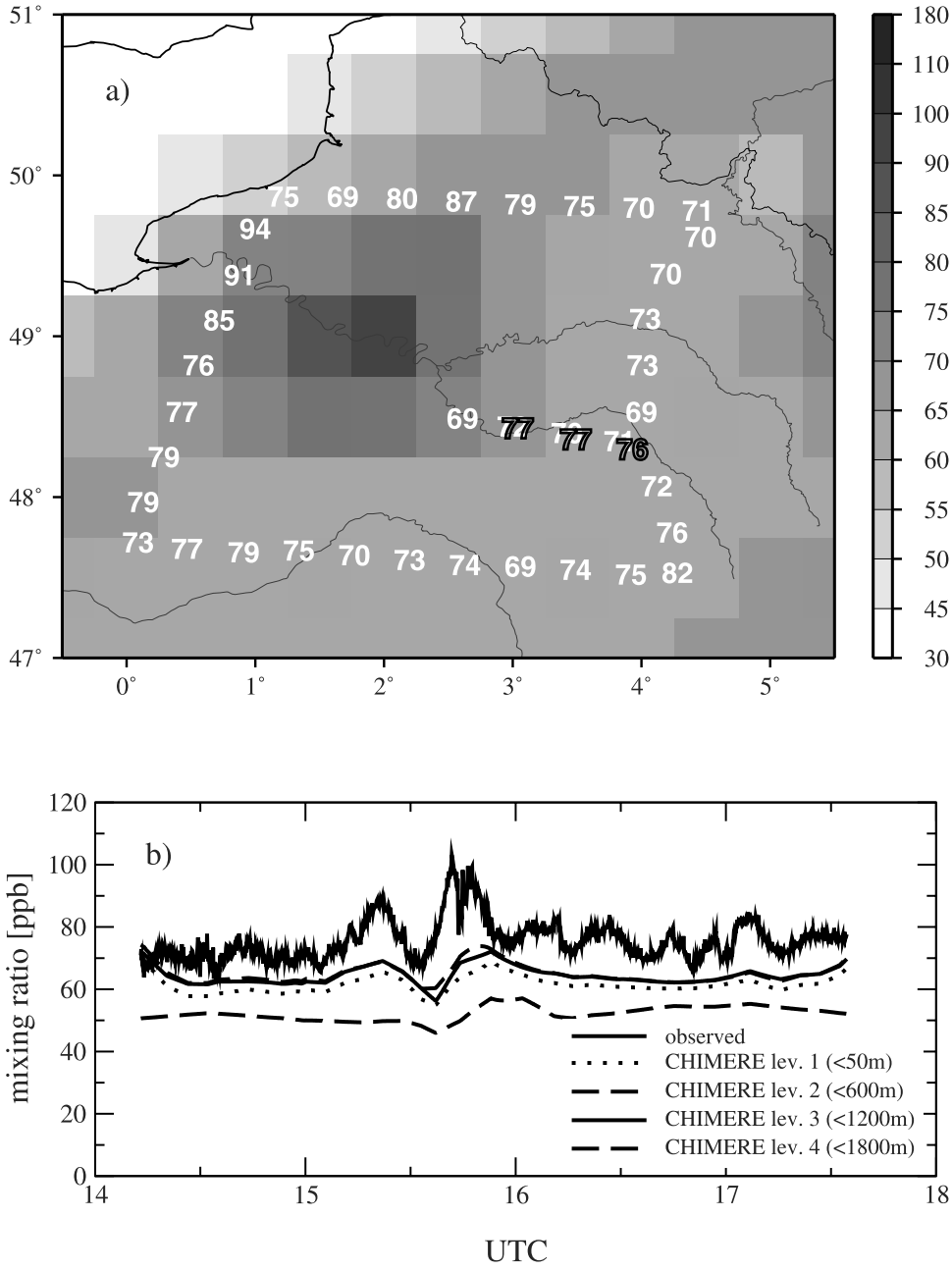

Figure 3. Comparison of simulated ozone mixing ratios with those observed by the Merlin IV aircraft during the flight on 17 July 1999. (a) The study area. White numbers indicate 5-min mean observed mixing ratios, and the grayscale gives the simulated field for 16 UTC. (b) Observations versus simulations for different model layers, interpolated in space and time. The flight starts in the center and is following the path in a counterclockwise direction.

estimations. Even the underestimated simulated ozone mixing ratios at the upwind leg of the flights are high, ~62 and ~75 ppb on 17 and 30 July, respectively. The adjoint sensitivities will be used to estimate the influence of different emitted species in different regions on these high values.

[27] To conclude the comparisons, it can be said that modeled and observed concentrations show a relatively high correlation, but there are cases of under- and overestimation. Therefore the adjoint sensitivities have to be interpreted with caution as far as the real world model is concerned. This is more so the case, as it is well known that models may sometimes simulate right concentrations for the wrong reasons. In this case, for example, results of emission reduction studies may be incorrect. Further sensitivity studies which cannot be detailed here suggest that major error sources besides the emission rates include uncertainties in the cloud cover, in reaction rates, and in boundary concentrations. Transport of trace gases should be reasonable despite the use of the simple advection scheme (see section 6.5). The relatively low time resolution of the meteorological input (3 hours) may cause problems in the

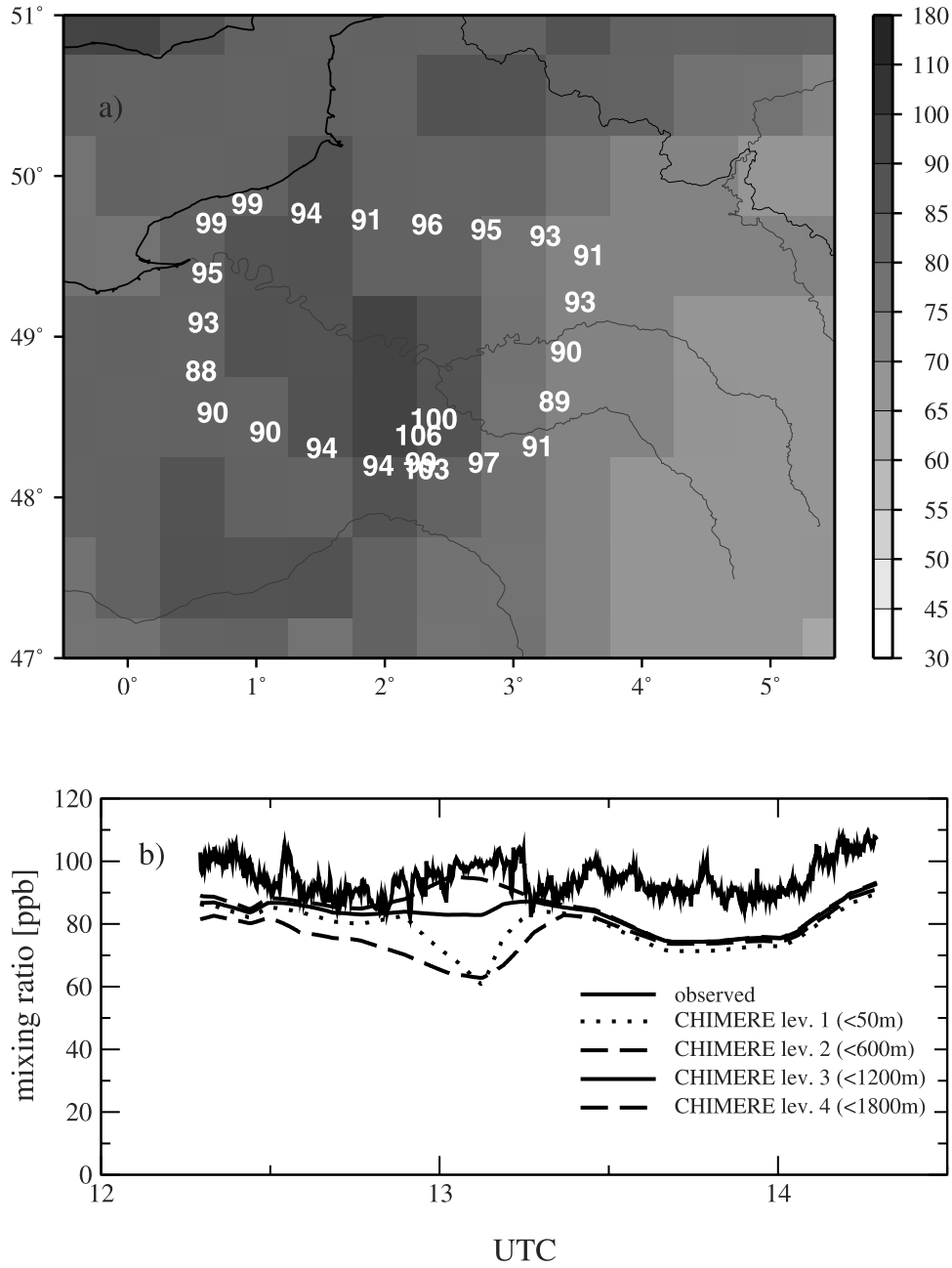

Figure 4. Same as in Figure 3, but for 30 July 1999. The simulated time in Figure 4a is 13 UTC, and the direction of the flight is clockwise.

morning hours if the growth of the boundary layer is mistimed.

6. Results of the Adjoint Sensitivity Calculations

[28] In this section, a selection of the results of the adjoint model integrations is presented. Two points regarding the limits of their interpretation should be recalled: (1) Owing to the nonlinearity of the model, the calculated gradients cannot be extrapolated to large changes of the parameters. Spot-checks with classical sensitivity calculations have shown that an extrapolation is reasonable in most cases for emission changes up to at least 10% (see section 6.5). (2) As in classical sensitivity studies, the results are subject to imperfections in the direct model formulation.

6.1. Geographical Distribution of Sensitivities to Emissions

[29] Figures 5a, 5b, and 5c show the sensitivity of the ozone mixing ratio in model layer 3 at the entrance of the Paris area to NO_x emissions from combustion for the target time 15 UTC on 17 July, for the target time 15 UTC on 30 July, and for the mean sensitivities of all 13 experiments of this series, respectively. The geographical distribution of the sensitivities reflects the trajectory of the air masses before arriving in the target box, the geographical distribution of

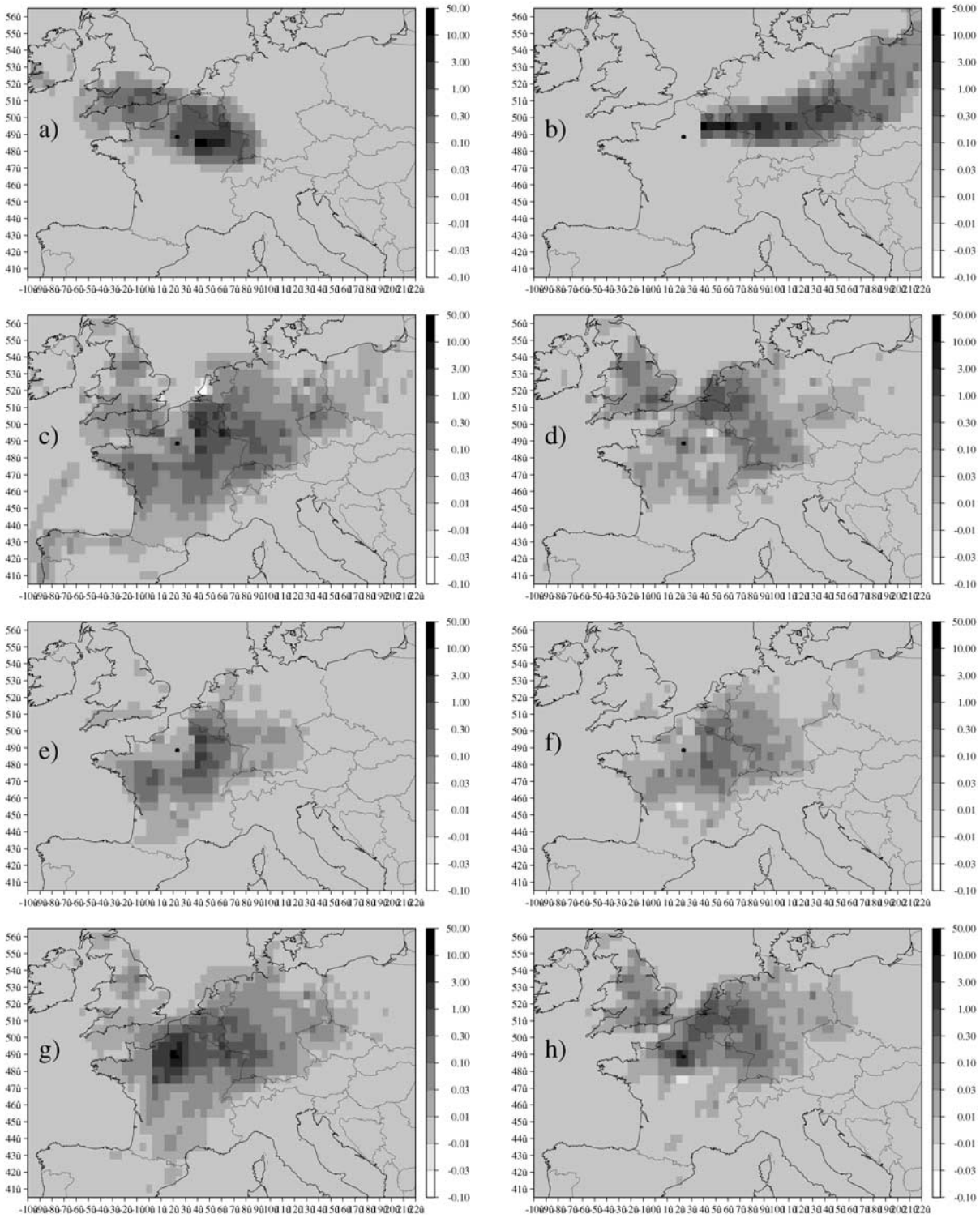

Figure 5. Sensitivity of ozone to emissions in each model grid box in ppt/% change of emissions. (a and b) Sensitivity to NO_x from combustion for 1999071715ENT3 and 1999073015ENT3, respectively. Figures 5c–5h show the mean of experiments 15ENT3: sensitivity to NO_x (c) from combustion and (e) from soils and to (d) anthropogenic and (f) biogenic volatile organic compounds (VOCs). (g and h) Mean sensitivity for the experiments 15EXT3 to NO_x from combustion and anthropogenic VOCs, respectively. All sensitivities are integrated over the complete simulation time.

the emissions, and the chemical transformation along the trajectory. Before entering the Paris area from the east on 17 July the air masses coming from the Atlantic have crossed the south of England and the north of France and then changed direction by nearly 180°. The ozone concentration has the highest sensitivities to emissions from the northeast of France, but also, high-emission areas in Belgium, London, and Paris itself are of influence. Please note (1) the logarithmic scale of the sensitivities and (2) that high-emission areas show, in general, high values as the sensitivities are expressed with respect to a relative and not an absolute emission change.

[30] The trajectory of the air masses entering the area on 30 July is completely different, leading to high sensitivities to emissions in a small part of the northeast of France, a west-east band of Germany which includes the Rhein-Main area, and the western part of the Czech Republic. Also, the sensitivities to some areas in Poland are not negligible. The mean pattern for 13 experiments shows that very different areas of western and central Europe may have an occasional influence on ozone concentrations of the air masses entering the Paris region. The highest mean sensitivities are discovered for the northeast of France, for Belgium, and for some areas in western Germany. As only 13 days are covered with experiments, this result cannot claim to be a climatological picture. However, summerly conditions and high ozone in Paris are frequently associated with easterly winds, and a real climatology might not look very different.

[31] The pattern of the mean sensitivity to anthropogenic VOC emissions (Figure 5d) differs from that to NO_x emissions. First, the amplitudes are, in general, lower, and second, the maxima are located at a larger distance to Paris, namely the high-emission areas Belgium/Netherlands/Rhein-Ruhr, and London. NO_x emissions in parts of these areas (except for Belgium) have a very low or, in certain grid boxes, even a negative influence. A sometimes sharp separation of areas with NO_x- and VOC-sensitive photochemistry can be stated. Figure 6b shows the sensitivity of ozone as a mean for the same experiments to an absolute change of anthropogenic VOC emissions. In this case the pattern is only influenced by the trajectories of the air masses and by the chemical regime. The pattern is much less structured than that for the relative emissions change (Figure 5d), which is strongly influenced by the distribution of the emissions in Europe as given in Figure 6a.

[32] Figures 5e and 5f show sensitivities to NO emissions from soils and from biogenic VOC emissions, respectively. In contrast to the direct anthropogenic sources, the large European agglomerations appear, of course, not as high sensitivity zones on the maps. NO emissions with the highest sensitivities have a French origin. This is partly caused by the inventory [*Stohl et al.*, 1996], which contains significantly higher NO emissions from soils for France than for, for example, Germany. In the case of biogenic VOC emissions the domination of French emissions is less pronounced.

[33] In order to illustrate the difference between air masses entering and leaving the Paris area, Figures 5g and 5h show mean sensitivities with respect to NO_x emissions from combustion and anthropogenic VOC emissions for the 13 experiments of the series 15EXT3. As expected, in contrast to Figures 5c and 5d, the sensitivity to emissions from the Paris area itself is very high. This is, again, more the case for NO_x than for VOC emissions. With our model resolution and the given emission inventories, afternoon ozone leaving the area seems to be more sensitive to NO_x than to VOCs.

6.2. Sensitivity to Different Emission Groups

[34] Table 2 quantifies the sensitivity of the ozone mixing ratio to the four emission groups of NO_x (from soils and combustion) and of VOCs (biogenic and anthropogenic) for all eight series of experiments. The sensitivities are integrated over all the simulation domain and time. For all series the sensitivity to NO_x emissions from combustion is about 3 times higher than from soils. Clearly, this ratio is largely dependent on the ratio of the respective emissions in the inventories. The domination of anthropogenic VOC emissions over biogenics is smaller, being of a factor of $\sim$1.5–2, depending on the experiment.

[35] The comparison of the direct anthropogenic emissions (only from combustion in the case of NO_x) shows that afternoon ozone entering or leaving the Paris area is significantly more sensitive to NO_x than to VOC emissions by a factor of $\sim$2.5. However, the sensitivity to VOCs at the ground level is slightly higher than in model layer 3. Regarding the different target boxes, one can state that the sensitivities for ozone downwind of Paris are $\sim$25% higher than for ozone upwind. The reasons for this are the larger total amount of emissions reaching the air masses which have already passed Paris and the, in general, higher influence of emissions closer to the target time.

[36] The picture changes completely for the experiments with the target time 9 UTC. On ground level the sensitivity of O_3 to NO_x emissions is negative. This is due to the titration of ozone by local NO emissions (representing $\sim$90% of total NO_x emissions) which is not compensated for by ozone production during nighttime. In model layer 3, which is decoupled from the surface layer in the nighttime as mostly only weak mixing occurs, the sensitivity to NO_x emissions remains positive and stronger than does the sensitivity to VOC emissions by a factor of 2.

[37] In a complementary study, *Schmidt* [2002] presents sensitivity calculations for the AOT40 value with respect to emissions for different regions of France. AOT40 is an integrated measure of ozone mixing ratios above 40 ppb during the daylight hours of one season. It is shown that in the Paris area, AOT40 is clearly more sensitive to changes in VOC emissions than to changes in NO_x emissions. This can be interpreted as an integrated measure of the sensitivities varying with the hour of the day.

[38] Regarding the results for single dates, sensitivities for 17 and 30 July, the dates considered in more detail in section 5, are close to the mean values; however, there is a slightly smaller influence of VOC emissions on both days and a stronger influence of NO_x from combustion for 30 July, whereas sensitivities for 9 August 1998, a very hot day in the Paris region, with temperatures up to 34°C and extremely high ozone concentrations (see Table 1), differ strongly from the mean results. NO_x emissions from soils reach a sensitivity of 70% of those from combustion. With respect to VOCs, ozone is even more sensitive to biogenic than to anthropogenic emissions. As the parameterizations for both emission types, NO_x from soils and biogenic

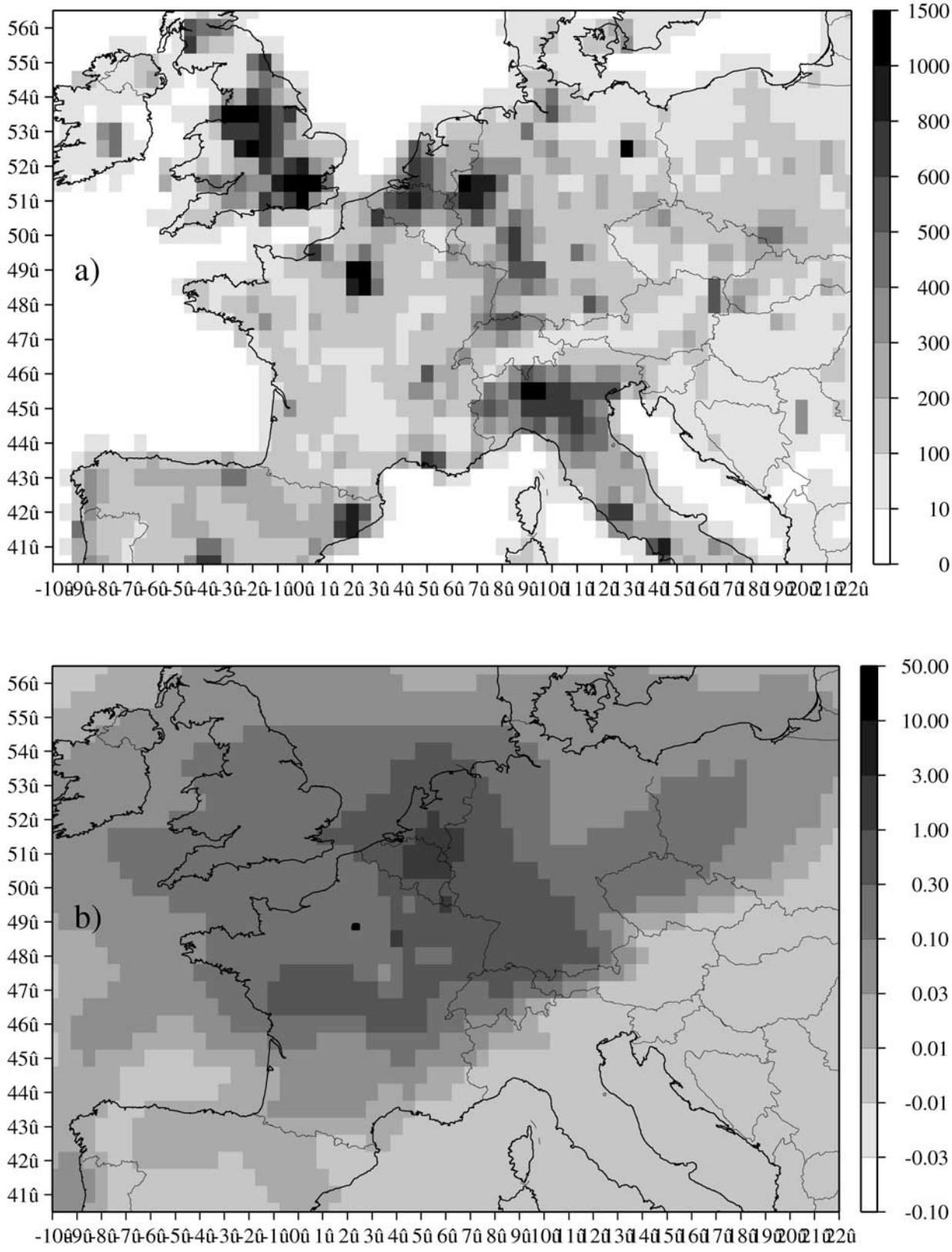

Figure 6. (a) Total mean weekday emissions of anthropogenic VOCs as used in CHIMERE for the month of July (in 10^9 molecules $(cm^2*s)^{-1}$). (b) Mean absolute sensitivity for the series of experiments 15ENT3 to anthropogenic VOC emissions (in ppt*(10^9 molecules $(cm^2*s)^{-1})^{-1}$). The sensitivities are integrated over the whole simulation time and are valid under the assumption that all eight anthropogenic model VOC species vary by this same amount.

Table 2. Sensitivities of Ozone to Four Emission Groups for Different Experiments in ppt/%

	Sensitivity to Emissions			
Experiment	NO_x (Combustion)	NO (Soil)	VOC (Anthropogenic)	VOC (Biogenic)
Mean 15ENT3	104	37	39	20
Mean 15ENT3[a]	58	25	6	6
Mean 15ENT1	105	39	45	27
Mean 15ENT1[a]	60	27	10	11
Mean 15EXT3	131	40	51	29
Mean 15EXT3[a]	73	26	9	8
Mean 15EXT1	132	41	59	38
Mean 15EXT1[a]	78	27	14	16
Mean 09ENT3	64	21	36	11
Mean 09ENT3[a]	24	11	5	1
Mean 09ENT1	−53	−22	74	84
Mean 09ENT1[a]	−70	−28	36	73
Mean 09EXT3	78	21	35	17
Mean 09EXT3[a]	30	11	4	3
Mean 09EXT1	−35	−17	86	74
Mean 09EXT1[a]	−57	−21	46	63
1998080815ENT3	127	46	52	44
1998080915ENT3	142	102	51	70
1999061615ENT3	144	25	83	15
1999061715ENT3	76	11	20	3
1999062515ENT3	107	22	74	5
1999062615ENT3	75	22	10	8
1999070215ENT3	74	39	13	12
1999071715ENT3	102	43	27	14
1999071815ENT3	91	63	28	32
1999072415ENT3	83	19	31	9
1999072515ENT3	72	26	73	17
1999072915ENT3	132	29	23	14
1999073015ENT3	130	36	22	13

[a]Value is integrated over 24 hours.

VOCs, include an exponential increase with temperature, the relatively high emissions should be responsible for the high sensitivities. Table 2 shows, also, that variations of the sensitivity to NO_x from combustion for the 13 different days are considerably smaller than for all other groups. The values vary between 74 and 142 and between 11 and 102 ppt% for NO_x from combustion and soils, respectively, and between 10 and 83 and between 3 and 70 ppt% for anthropogenic and biogenic VOCs, respectively.

6.3. Timescale of the Influence of Emissions

[39] The geographical distribution of sensitivities (Figure 5) shows that the influence of VOC emissions is spatially more extended than is the influence of NO_x emissions. As larger distances from the target region imply longer transport times, this is confirmed in Figure 7, which shows sensitivities integrated over the whole model domain and accumulated in time. While the sensitivity to NO_x emissions, both from combustion and soils, is growing rapidly during the first hours before the target time, the sensitivity to VOC emissions remains relatively low during the first 24 hours. Table 2 shows that NO_x emissions during the first 24 hours account for ~60% of the total sensitivity of afternoon ozone. For VOC emissions, this value is only ~20%. To explain this behavior, Figure 8 shows the time evolution of the sensitivities to the most important emitted VOC model species. Mean sensitivities of ozone upwind of Paris in model layer 3 to several species (acetaldehyde, α-pinene, and O-xylene) are even negative during the first hours before the target time. A product of different reactions of these species is the acetyl peroxy radical, of which the principal reactions are those with NO_x: $CH_3CO_3 + NO \rightarrow NO_2 + CH_3O_2 + CO_2$ and $CH_3CO_3 + NO_2 \rightarrow PAN$. Under certain conditions, in particular with a very high NO_2 to NO ratio as it is given, for example, in the region relatively far from fresh emissions upwind of Paris, the latter reaction can be dominating. NO_2 is thereby temporarily removed from the system, and O_3 production is reduced on a short timescale.

[40] The time evolution of the sensitivities can also vary significantly depending on the trajectory of the air masses. In Figure 7 it is shown that ozone in experiment 1999073015ENT3 is much more sensitive to NO_x emissions on day 1 than it is in experiment 1999071715ENT3. This is due to the air mass in the first case crossing high-emission areas in Germany. Contrarily, in the second case the sensitivity to VOC emissions grows on day 2 as a consequence of emissions in the London area. In all cases shown in this figure the sensitivity to emissions on day 3 is weak, which shows that, in general, ozone has a short "memory" of emissions lasting only several days, and it should not be necessary to extend the integration time of the experiments.

6.4. Interpretation of the Sensitivities With Respect to the Ozone Reduction Potential

[41] Summing up the sensitivities for all four emission types discussed in section 6.2, one obtains a sensitivity of 0.200 ppb for a 1% emission change as a mean for the 15ENT3 experiments (see Table 2). This value is of the same order as for the experiments of 17 and 30 July (0.186 and 0.201, respectively), but the value for 9 August 1998 is significantly higher (0.363 ppb%), and the value is also higher for air masses leaving Paris at this altitude level

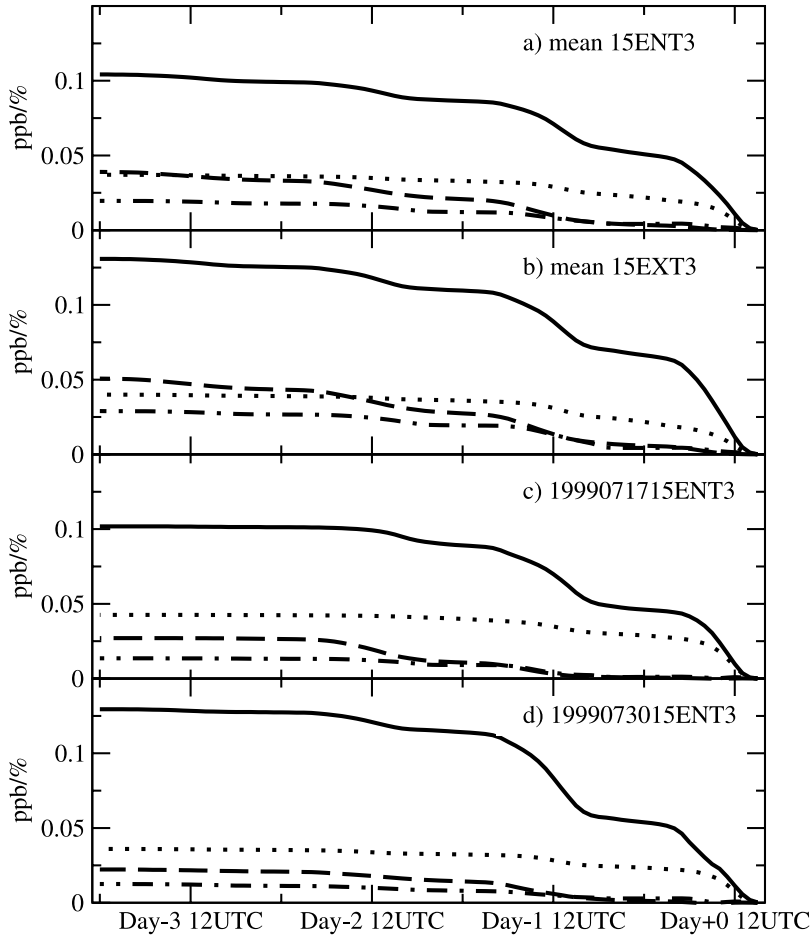

Figure 7. Sensitivity of ozone to emissions of NO_x from combustion (solid line) and from soils (dotted line) and of anthropogenic (dashed line) and biogenic (dash-dotted line) VOCs: (a) mean 15ENT3; (b) mean 15EXT3; (c) 1999071715ENT3; and (d) 1999073015ENT3. Sensitivities are accumulated backward in time, i.e., a value given for, for example, day 1 at 12 UTC indicates the change of the ozone mixing ratio at the target time day +0 at 15 UTC caused by a 1% change of emissions during the 27 hours in between.

(0.251 ppb% on average). A value of 0.2 ppb% means that an emission uncertainty of 10% would lead to an uncertainty of the ozone mixing ratio of 2 ppb. The model underestimation of ozone upwind of Paris observed on 17 and 30 July is ~10 ppb. Though emissions are frequently estimated to have errors of the order of 50%, and though nonlinear responses on emission changes of this magnitude have to be expected, it does not seem very likely that only errors in the emission rates are responsible for these errors.

[42] With respect to the uncertainty introduced by the different groups of emissions, it is necessary to have separate error estimations. *Hanna et al.* [1998] estimate a 95% uncertainty range for NO_x emissions from combustion as lying between 30 and 40%, for anthropogenic VOCs between 50 and 80%, and for NO_x from soils and biogenic VOCs by a factor of 2. A multiplication of these estimations with the sensitivities for the groups given in Table 2 leads to uncertainties of the model results of the same order of magnitude for all groups.

[43] Assuming that the model gives a realistic picture of the real world, the sensitivities can also be interpreted with respect to the effect of emission reductions. A 10% reduction

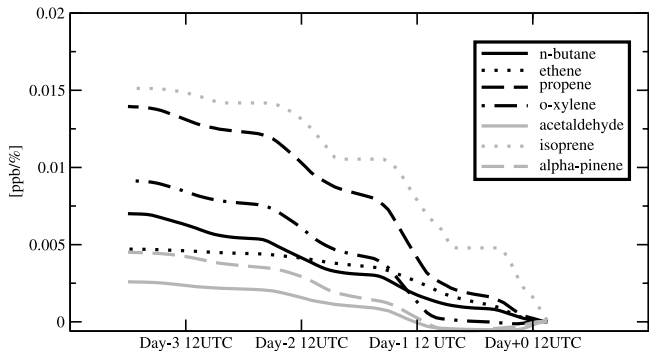

Figure 8. Sensitivity of ozone to emissions of different VOCs as a mean value of the experiments 15ENT3. Sensitivities are accumulated backward in time. Note that real VOC species are aggregated to model species. The VOC names given in the legend are, therefore, only indicating a representative group of VOCs with similar reaction characteristics.

Table 3. Comparison of Sensitivities of Ozone to Emission Changes of NO_x in the Complete Model Area for First-Order and Piecewise Parabolic Method (PPM) Convection Schemes[a]

Advection Scheme	ϵ	Sensitivity, ppt/%
First-order	0	166.5
First-order	0.01	162.2
First-order	0.1	156.7
PPM	0	158.3
PPM	0.01	153.1
PPM	0.1	145.8

[a]Results are given for experiment 19990730ENT3 and are computed with the adjoint method ($\epsilon = 0$) and with emission perturbations of 1% and 10% ($\epsilon = 0.01$ and $\epsilon = 0.1$, respectively).

of the direct and indirect anthropogenic emissions would lead to an ozone reduction of 1.8 ppb in the mean in the third model layer upwind of Paris and downwind to a reduction of 2.3 ppb. For short-term reductions during only 24 hours before the target time, this would reduce to 0.9 and 1.1 ppb, respectively. As already discussed in section 6.2, NO_x reductions would be significantly more effective than would be those of VOCs. However, NO_x reductions of a large amount would probably change the chemical regime, and VOC reductions would become more effective. For such cases the interpretation of the calculated sensitivities is clearly limited.

6.5. Comparison of Results Obtained With Different Advection Schemes

[44] The application of the diffusive first-order advection scheme instead of the PPM scheme is supposed to cause errors in the sensitivity calculations. Two types of experiments are performed to estimate this problem. Table 3 presents sensitivities of ozone in experiment 19990730ENT3 to a variation of the total NO_x emissions in the complete model domain. The sensitivities are computed with both the adjoint method and the perturbation approach. Results for the two advection schemes are very similar, which means that the errors for this type of result should be <10%. The similar results for adjoint and perturbation computations indicate that the nonlinearity of the PPM scheme is also not influencing the results significantly.

[45] The same type of test is performed for sensitivities to emission changes in single grid boxes which give a north-south cross section through the "plume" of high sensitivities for experiment 19990730ENT3 (see Figure 5b). Results are presented in Figure 9 and show that the choice of the advection scheme is not influencing the location of the areas with high sensitivities but rather the amplitude. Sensitivities are probably underestimated in these areas due to the diffusivity of first-order advection. However, the occurrence of nonphysical negative sensitivities shows the problems of the PPM scheme. Sensitivities computed with a 50% perturbation indicate that nonlinear effects are very small for both schemes at this distance from the target box. Strong nonlinearities can be observed for the PPM scheme and for grid boxes close to the target (not shown in Figure 9).

7. Summary and Discussion

[46] An adjoint model of the Eulerian chemistry transport model CHIMERE, which covers the European boundary layer, has been developed. This study was intended to show the utility of such a model for the calculation of sensitivities of the model result to model parameters, in this case the sensitivity of ozone concentrations to emissions on the European scale. The model was applied to study 13 cases of elevated ozone concentrations in the Paris region during the summer seasons of 1998 and 1999 in order to better understand the sources of photochemical air pollution in this area and to facilitate the interpretation of the measurements of the ESQUIF campaign. In the following paragraphs the main results will be recapitulated and discussed.

[47] A large number of modeling studies have already addressed the question of whether NO_x or VOC control would be more effective in the reduction of photochemical pollution. A comparison study [*Hass et al.*, 1997] with four different European models suggests that, in general, NO_x control would reduce regional ozone more effectively. Several studies for the U.S. confirm this but point out that in high-emission areas, ozone might be more sensitive to VOC emissions [see e.g., *Roselle and Schere*, 1995; *Russell and Dennis*, 2000, and references therein]. *Menut et al.* [2000b], with an adjoint of a simplified local model for Paris, show that peak ozone concentrations may be both NO_x- or VOC-sensitive, depending on meteorological conditions. Our results confirm for all 13 days that maximum ozone values at ~100 km distance of Paris are more sensitive to changes of NO_x emissions than to changes of VOC emissions. The adjoint model allows a differentiation of this result with respect to the location and time of the emissions. In the mean case, ozone entering the Paris region is most sensitive to NO_x emissions in the northeastern part of France, in Belgium, and in parts of western Germany but with a strong variation from case to case. Regarding VOC emissions, the highest sensitivities are detected for regions more distant from Paris, in particular the high-emission areas Belgium/Netherlands/Rhein-Ruhr and London. The spatial distance is also reflected in the timescale of the sensitivities. While >50% of the total sensitivity to NO_x is caused by emissions during the 24 hours before the target time, in the case of VOCs these emissions account for only

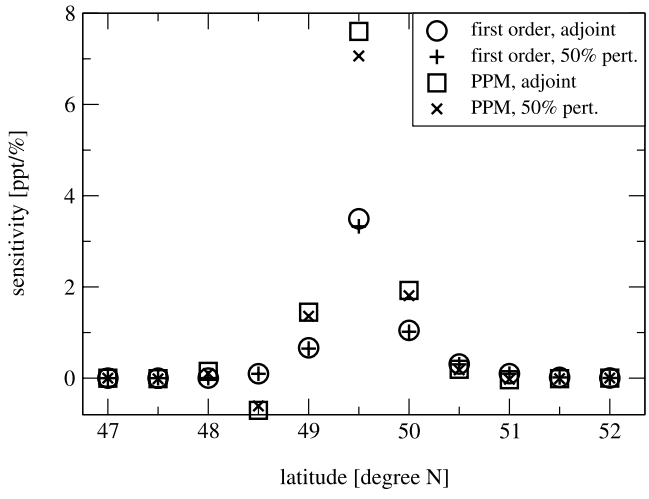

Figure 9. Sensitivity of ozone for the experiment 1999073015ENT3 to total NO_x emission changes in model grid boxes with their centers at latitudes indicated by the x axis and at the longitude 11°E. Sensitivities are calculated for first-order and piecewise parabolic method advection with both the adjoint and the perturbation method.

~20% of the sensitivity. The NO_x/VOC sensitivities are very similar for ozone downwind of Paris even if the absolute values are higher due to the recent crossing of the high-emission Paris area. It should be noted that in these cases the interpretation might suffer from an insufficient resolution of the city plume.

[48] Concerning the relative importance of anthropogenic versus biogenic VOCs, it can be stated that the sensitivity to the anthropogenic emissions is on average larger by a factor of 2, whereas during the first 24 hours, while the air masses are passing mostly rural areas, the influence of both types of emissions is of the same size. Owing to the relatively small amount of NO_x emissions from soils, these emissions have, in general, a significantly smaller influence than do emissions from combustion. However, taking into account the large uncertainty associated with soil emissions, both types of emissions cause uncertainties in the model's ozone response of the same order of magnitude. This is also true for VOC emissions and shows that attempts to improve simulations by improving emission inventories should focus on all four types of emissions.

[49] Limits for the interpretation of the adjoint sensitivities in the context of emission reduction scenarios have been discussed in detail. However, the problem of model deficiencies possibly changing sensitivities to emissions is also valid for classical sensitivity studies. For small changes of emissions the adjoint sensitivities should give a good estimation of the model response. This study shows that during photochemical pollution episodes a 10% reduction of anthropogenic emissions would reduce ozone upwind of Paris by <2 ppb on average. Regarding attempts to reduce peak concentrations by short-term emission reductions, it is important to note that the effect would be less than half of that if emissions are reduced only during 24 hours. The adjoint approach offers a big advantage by regarding in detail the influence of different species emitted at different locations and times. However, if large reductions are the subject of the study, the results should be verified by less differentiated classical studies.

[50] The relatively small model response of a ~2 ppb change of the ozone mixing ratio to a 10% change of emissions might give important hints in the search for modeling errors which are frequently of the order of 10 ppb. It seems not very likely that they are caused by errors in emission rates only. During the adjoint model integrations presented here, sensitivities were calculated not only with respect to emissions but also with respect to other model parameters such as reaction rates and meteorological parameters. The results indicate that the uncertainties of numerous different model parameters might cause model errors of the same order of magnitude as emissions. The results will be presented in more detail in a future study.

[51] **Acknowledgments.** The authors would like to thank R. Vautard, LMD, Palaiseau, France, and L. Menut, LISA, Creteil, France, for many helpful discussions. The French aircraft team from Météo France/CAM is acknowledged for their efforts concerning the aircraft observations. Financial support was provided by the TOTAL-FINA-ELF company.

References

Atmospheric Pollution Over the Paris Area Project Team (ESQUIF), Etude et simulation de la qualité de l'air en ile de France, *Final Rep.*, Inst. Pierre Simon Laplace, Paris, 2001.

Carpenter, R. L., Jr., K. K. Droegemeier, P. R. Woodward, and C. E. Hane, Application of the piecewise parabolic method (PPM) to meteorological modeling, *Mon. Weather Rev.*, *118*, 586–612, 1990.

Chao, W. C., and L.-P. Chang, Development of a four-dimensional variational analysis system using the adjoint method at GLA. part 1: Dynamics, *Mon. Weather Rev.*, *120*, 1661–1673, 1992.

Cho, S. T., G. R. Carmichael, and H. Rabitz, Sensitivity analysis of the atmospheric reaction diffusion equation, *Atmos. Environ.*, *21*, 2589–2598, 1987.

Daley, R., *Atmospheric Data Analysis*, Cambridge Univ, Press, New York, 1991.

Elbern, H., and H. Schmidt, A four-dimensional variational chemistry data assimilation scheme for Eulerian chemistry transport modeling, *J. Geophys. Res.*, *104*, 18,583–18,598, 1999.

Elbern, H., and H. Schmidt, Ozone episode analysis by four-dimensional variational chemistry data assimilation, *J. Geophys. Res.*, *106*, 3569–3590, 2001.

Elbern, H., H. Schmidt, and A. Ebel, Variational data assimilation for tropospheric chemistry modeling, *J. Geophys. Res.*, *102*, 15,967–15,985, 1997.

Elbern, H., H. Schmidt, O. Talagrand, and A. Ebel, 4D-variational data assimilation with an adjoint air quality model for emission analysis, *Environ. Modell. Software*, *15*, 539–548, 2000.

Erisman, J. W., W. van Pul, and G. Wyers, Parameterization of surface resistance for the quantification of atmospheric deposition of acidifying pollutants and ozone, *Atmos. Environ.*, *28*, 2595–2607, 1994.

Fisher, M., and D. J. Lary, Lagrangian four-dimensional variational data assimilation of chemical species, *Q. J. R. Meteorol. Soc.*, *121*, 1681–1704, 1995.

Gao, D., W. R. Stockwell, and J. B. Milford, First-order sensitivity and uncertainty analysis for a regional-scale gas-phase chemical mechanism, *J. Geophys. Res.*, *100*, 23,153–23,166, 1995.

Generation of European Emission Data for Episodes Project (GENEMIS), *EUROTRAC Annual Report 1993*, part 5, EUROTRAC Int. Sci. Secr., Garmisch-Partenkirchen, Germany, 1994.

Giering, R., and T. Kaminski, Recipes for adjoint code construction, *Assoc. Comput. Mach. Trans. Math. Software*, *24*, 437–474, 1998.

Guenther, A., Seasonal and spatial variations in the natural volatile organic compound emissions, *Ecol. Appl.*, *7*, 34–45, 1997.

Hanna, S. R., J. C. Chang, and M. E. Fernau, Monte Carlo estimates of uncertainties in predictions by a photochemical grid model (UAM-IV) due to uncertainties in input variables, *Atmos. Environ.*, *32*, 3619–3628, 1998.

Hass, H., P. J. H. Builtjes, D. Simpson, and R. Stern, Comparison of model results obtained with several European regional air quality models, *Atmos. Environ.*, *31*, 3259–3279, 1997.

Hauglustaine, D. A., G. P. Brasseur, S. Walters, P. J. Rasch, J.-F. Müller, L. K. Emmons, and M. A. Carroll, MOZART: A global chemical transport model for ozone and related chemical tracers: 2, Model results and evaluation, *J. Geophys. Res.*, *103*, 28,291–28,336, 1998.

Lattuati, M., Contribution à l'étude du bilan de l'ozone troposphérique à l'interface de l'Europe et de l'Atlantique Nord: Modélisation lagrangienne et mesures en altitide, Ph.D. thesis, Univ. Paris 6, France, 1997.

Lewis, J. M., and J. C. Derber, The use of adjoint equations to solve a variational adjustment problem with advective constraints, *Tellus, Ser. A*, *37*, 309–322, 1985.

Marchuk, G. I., *Numerical Methods in Weather Prediction*, Academic, San Diego, Calif., 1974.

Menut, L., et al., Measurements and modeling of atmospheric pollution over the Paris area: An overview of the ESQUIF project, *Ann. Geophys.*, *18*, 1467–1481, 2000a.

Menut, L., R. Vautard, M. Beekmann, and C. Honoré, Sensitivity of photochemical pollution using the adjoint of a simplified chemistry-transport model, *J. Geophys. Res.*, *105*, 15,379–15,402, 2000b.

Middleton, P., W. R. Stockwell, and W. P. L. Carter, Aggregation and analysis of volatile organic compound emissions for regional modeling, *Atmos. Environ.*, *24*, 1107–1133, 1990.

Mylona, S., EMEP emission data: Status report 1999, *Note 1/99*, Eur. Monit. Eval. Programme Meteorol. Syn. Cent. West, Oslo, 1999.

O'Brien, J. J., A note on the vertical structure of the eddy exchange coefficient in the planetary boundary layer, *J. Atmos. Sci.*, *27*, 1213–1215, 1970.

Roselle, S. J., and K. L. Schere, Modeled response of photochemical oxidants to systematic reductions in anthropogenic volatile organic compound and NO_x emissions, *J. Geophys. Res.*, *100*, 22,929–22,941, 1995.

Russell, A., and R. Dennis, NARSTO critical review of photochemical models and modeling, *Atmos. Environ.*, *34*, 2283–2324, 2000.

Schmidt, H., Vierdimensionale Datenassimilation nach der Variationsmethode für ein mesoskaliges Chemietransportmodell, Ph.D. thesis, Inst. für Geophys. und Meteorol., Univ. zu Köln, Germany, 1999.

Schmidt, H., Sensitivity studies with the adjoint of a chemistry transport model for the boundary layer, in *Air Pollution Modelling and Simulation*, edited by B. Sportisse, pp. 400–410, Springer-Verlag, New York, 2002.

Schmidt, H., C. Derognat, R. Vautard, and M. Beekmann, A comparison of simulated and observed ozone mixing ratios for the summer of 1998 in western Europe, *Atmos. Environ.*, *35*, 6277–6297, 2001.

Seinfeld, J. H., and S. N. Pandis, *Atmospheric Chemistry and Physics*, Wiley-Interscience, New York, 1998.

Simpson, D., Long period modelling of photochemical oxidants in Europe: Calculations for July 1985, *Atmos. Environ.*, *26*, 1609–1634, 1992.

Simpson, D., et al., Inventorying emissions from nature in Europe, *J. Geophys. Res.*, *104*, 8113–8152, 1999.

Sirkes, Z., and E. Tziperman, Finite difference of adjoint or adjoint of finite difference?, *Mon. Weather Rev.*, *125*, 3373–3378, 1997.

Stohl, A., E. Williams, G. Wotawa, and H. Kromp-Kolb, A European inventory of soil nitric oxide emissions and the effect of these emissions on the photochemical formation of ozone, *Atmos. Environ.*, *30*, 3741–3755, 1996.

Talagrand, O., The use of adjoint equations in numerical modelling of the atmospheric circulation, in *Proceedings of the Workshop on Automatic Differentiation of Algorithms: Theory, Implementation and Application*, edited by A. Griewank and G. G. Corliss, pp. 169–180, Soc. for Ind. and Appl. Math., Philadelphia, Pa., 1991.

Talagrand, O., and P. Courtier, Variational assimilation of meteorological observations with the adjoint vorticity equation. I: Theory, *Q. J. R. Meteorol. Soc.*, *113*, 1311–1328, 1987.

Thuburn, J., and T. W. N. Haine, Adjoints of nonoscillatory advection schemes, *J. Comp. Phys.*, *171*, 616–631, 2001.

Vautard, R., M. Beekmann, L. Menut, and M. Lattuati, Application of adjoint modelling in urban pollution, in *Proceedings of the EUROTRAC Symposium 98*, vol. 2, edited by P. M. Borrell and P. Borrell, 502–508, WIT Press, Boston, Mass., 1999.

Vautard, R., M. Beekmann, J. Roux, and D. Gombert, Validation of a deterministic forecasting system for the ozone concentrations over the Paris area, *Atmos. Environ.*, *35*, 2449–2461, 2001.

Veldkamp, E., and M. Keller, Fertilizer-induced nitric oxide emissions from agricultural soils, *Nutrient Cycling Agroecosystems*, *48*, 69–77, 1997.

Verwer, J. G., Gauss-Seidel iteration for stiff ODEs from chemical kinetics, *SIAM J. Sci. Comput.*, *15*, 1243–1250, 1994.

Vestreng, V., and E. Storen, Analysis of UNECE/EMEP emission data: MSC-W status report 2000, *Note 1/00*, Eur. Monit. Eval. Programme Meteorol. Syn. Cent. West, Oslo, 2000.

Vukićević, T., and P. Hess, Analysis of tropospheric transport in the Pacific Basin using the adjoint technique, *J. Geophys. Res.*, *105*, 7213–7230, 2000.

Vukićević, T., M. Steyskal, and M. Hecht, Properties of advection algorithms in the context of variational data assimilation, *Mon. Weather Rev.*, *126*, 1221–1231, 2001.

Wesely, M. L., and B. B. Hicks, Some factors that affect the deposition rates of sulfur dioxide and similar gases on vegetation, *J. Air Pollut. Control Assoc.*, *27*, 1110–1116, 1977.

Williams, E. J., G. L. Hutchinson, and F. C. Fehsenfeld, NO_x and N_2O emissions from soil, *Global Biogeochem. Cycles*, *6*, 351–388, 1992.

D. Martin, Météo France, Direction Générale/Environnnement Atmosphérique, 1 Quai Branly, 75007 Paris, France. (daniel.martin@meteo.fr)

H. Schmidt, Max-Planck-Institute for Meteorology, Bundesstrasse 55, 20146 Hamburg, Germany. (hauke.schmidt@dkrz.de)